

Flow reproducibility of whole blood and other bodily fluids in simplified no reaction lateral flow assay devices

H. Li,¹ D. Han,¹ M. A. Hegener,² G. M. Pauletti,² and A. J. Steckl^{1,a)}

¹Nanoelectronics Laboratory, Department of Electrical Engineering and Computing Systems, University of Cincinnati, Cincinnati, Ohio 45221, USA

²Winkle College of Pharmacy, University of Cincinnati, Cincinnati, Ohio 45267, USA

(Received 11 January 2017; accepted 24 March 2017; published online 7 April 2017)

The “no reaction” lateral flow assay (nrLFA) uses a simplified LFA structure with no conjugate pad and no stored reagents. In the nrLFA, the capillary-based transport time or distance is the key indicator, rather than the outcome of a biochemical reaction. Hence, the calibration and reproducibility of the nrLFA device are critical. The capillary flow properties of several membrane types (nitrocellulose, nylon, cellulose acetate, polyethersulfone, and polyvinylidene difluoride) are evaluated. Flow rate evaluations of MilliporeSigma Hi-Flow™ Plus (HF075, HF135 and HF180) nitrocellulose membranes on nrLFA are performed using bodily fluids (whole blood, blood plasma, and artificial sweat). The results demonstrate that fluids with lower viscosity travel faster, and membranes with slower flow rate exhibit higher capability to distinguish fluids with different viscosities. Reproducibility tests of nrLFA are performed on HF075, demonstrating excellent reproducibility. The coefficient of variation for blood coagulation tests performed with the nrLFA using induced coagulation was 5% for the plasma front and 2% for the RBC front. The effects of variation in blood hematocrit and sample volume are also reported. The overall results indicate that the nrLFA approach has a high potential to be commercially developed as a blood monitoring point-of-care device with simple calibration capability and excellent reproducibility. *Published by AIP Publishing.* [<http://dx.doi.org/10.1063/1.4979815>]

I. INTRODUCTION

Lateral flow (immuno)assay (LFA) technology is used to fabricate simple, portable, and low-cost detection devices for applications in biomedicine, agriculture, food and environmental sciences, such as tumor biomarkers,¹ microorganisms,² toxins,³ heavy metals,⁴ and pesticides.⁵ Lateral flow takes place in porous membranes through which fluid samples are transported via the capillary effect. The structure (pore size, tortuosity, etc.) and composition (material substrate, density, surface additives, etc.) can be selected to enable flow of components ranging from ions (a few nanometers) and small molecules (tens of nanometers), to proteins to cells (several micrometers). Conventional cellulose-based paper is attractive for many assays because of its low cost and ease of disposal. However, proteins do not adsorb well on cellulose and cellulose acetate (CA), limiting their scope in immunoassays which require protein immobilization.⁶ Nitrocellulose (NC) is a modified form of cellulose produced by treating cellulose with nitric acid resulting in the replacement of the hydroxyl group with nitrate groups. NC is hydrophobic and membranes made from pure NC do not wet aqueous solutions. To enable wetting, surfactants are incorporated during the membrane fabrication process.⁷ NC-based membranes are employed in LFAs because of their high binding ability to proteins and other important biomolecules.⁸

^{a)} Author to whom correspondence should be addressed. Electronic mail: a.steckl@uc.edu

The seminal work^{9,10} of the Whitesides group in fabricating paper-based microfluidic devices that typically involve non-immunological reactions for colorimetric detection has defined an even simpler approach for easy, rapid, and low-cost diagnostic tests. This has resulted in the development of microfluidic paper-based analytical devices (μ PADs), which typically consist of laminated paper strips.^{11–20} These devices use lateral (and occasionally vertical) flow in paper to screen for various medical conditions relevant to human and animal health, environmental monitoring, and food safety. The low cost of paper and other materials utilized in μ PAD fabrication encourages broader application and more frequent usage, and their disposable nature minimizes the risk of cross contamination between tests. Recently, paper-based devices have also been reported for various electronic applications^{21–25} including chemical and biological sensors and biofuel cells. Numerous sensing and fabrication methods^{26–32} and network geometry^{33–38} of paper devices have been developed, giving paper-based microfluidic devices great potential for applications in semi-quantitative multi-step assays.

We have pursued a simplified LFA version that does not involve biochemical reactions, which we have named *no reaction lateral flow assay* (nrLFA). The nrLFA uses capillary flow properties of the fluid to be analyzed to determine its rheological properties. This represents a significant advantage but requires that (1) the fluid is colored to enable visual detection and (2) that its rheological properties are significantly changed by a medical condition. We have previously reported the use of nrLFA for point-of-care (POC) blood coagulation monitoring.³⁹ Most frequently, health status assessment of an individual requires blood analysis. Comprehensive blood tests that involve collection of a blood sample and subsequent analysis for desired health parameters are typically performed in a hospital or laboratory setting. Many tests require 2–5 ml of blood, which is obtained with venous puncture. In recent years, there has been a continuing effort to develop POC tests to measure a variety of biochemical blood parameters, such as glucose, hemoglobin, lactate, and ions.⁴⁰ These POC blood tests can effectively be completed using a much smaller capillary blood volume ($\sim 1\text{--}25\ \mu\text{l}$ (Ref. 40)) obtained by a finger prick with a lancet and utilize optical or electrochemical methods⁴¹ for detection. The price of commercial POC blood analyzers ranges from \$1 to \$125 per test (depending on whether it uses a simple strip, a cuvette, or a cartridge) and \$230 to \$5,500 for the typical reader unit (more information can be found in Table SI in the [supplementary material](#)).

A comparison of the attributes of the nrLFA device and commercial POC blood analyzer is shown in Fig. 1. For whole blood (WB) assays, the nrLFA exhibits key features, such as a simple device structure (simplified LFA structure rather than a complicated electronic device), simple fabrication process, low cost (affordable POC test without the need for an expensive analyzer unit), easy operation, and long shelf life due to no pre-stored reagents in the device. These attributes together with potential future smartphone diagnosis apps make nrLFA an ideal device in resource-limited settings without the need for expensive instruments and for patient self-testing at home without a trip to physician's office. However, nrLFA also poses some challenges that need to be investigated, such as the effect of secondary properties (pH, polarity, etc.) of the fluid being measured and critical dependence on the reproducible flow rate and material properties.

The “signal” in the nrLFA device is related to the distance traveled by the fluid (or any of its components) in a given time, or conversely the time required for the fluid to reach a certain point in the strip. Therefore, the calibration and reproducibility of fluid flow in the device are critical for reliable operation. Chromatography paper has already been proven to exhibit precise capillary flow and can potentially be used as a viscometer.⁴² Generally, in commercial NC membranes, there are flow rate variations between rolls within a cast lot and between cast lots, due to inherent variation in the casting process. This indicates the importance of flow rate calibration when first receiving the set of membrane materials in order to ensure that the flow properties of the membranes are fully characterized and calibrated before utilizing them for tests.

In this article, the reproducibility of the nrLFA device when using various membranes with several sample fluids, including anti-coagulated whole blood and blood plasma, is reported. In order to isolate the effect of membrane reproducibility, we have used laboratory-grade blood samples from the same vendor. In the future, we will investigate the effects of blood sample variability (from both healthy subjects and patients) on the nrLFA performance.

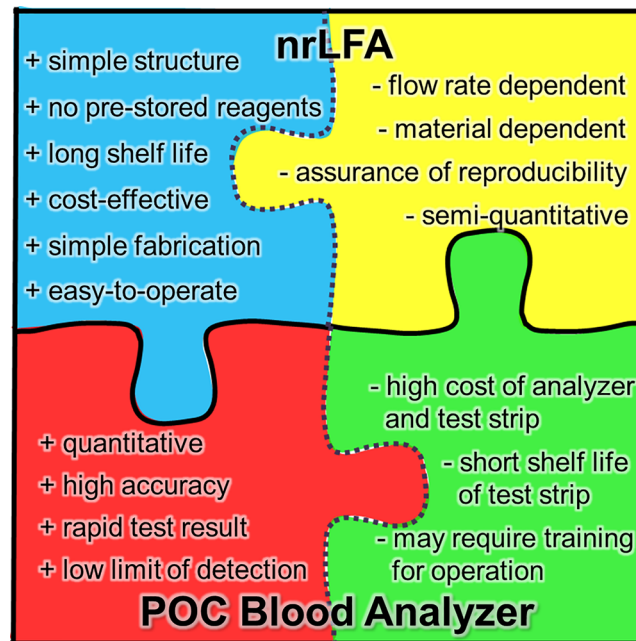


FIG. 1. Comparison of attributes of the nrLFA device and commercial POC blood analyzer.

Whole blood is an essential body fluid that gives significant insight of an individual's health conditions. Blood makes up $\sim 7\%$ of an individual's total body weight and contains approximately 45% (v/v) of cellular components, including erythrocytes (red blood cells—RBCs), leukocytes (white blood cells—WBCs) and thrombocytes (platelets). More than 99% of the cells in blood are RBCs.⁴³ The remaining 55% (v/v) of whole blood consists of a protein-rich plasma, with 92% (w/w) water and 7% dissolved proteins (such as albumin, globulins, and fibrinogen). The remaining 1% consists of dissolved organic molecules (e.g., amino acids, glucose, and lipids), dissolved gases such as O_2 and CO_2 , ions (e.g., Na^+ , K^+ , Cl^- , and Ca^{2+}), as well as trace elements and vitamins.⁴⁴ Abnormality in whole blood viscosity can be an early indicator of cardio- or cerebro-vascular diseases, diabetes mellitus, and liver diseases.⁴⁵ Furthermore, low RBC count in patients undergoing chemotherapy can indicate chemotherapy-induced anemia. Unlike the conventional test method where RBCs are removed and only plasma is utilized for diagnostics,^{46–49} whole blood can be directly applied onto our nrLFA device since we utilize the transport of RBCs as a color indicator of rheological properties of whole blood, which are related to the individual's blood coagulation condition.

The rheology of blood flow in the body is very complex. Blood can be considered a two-phase suspension⁵⁰ of formed elements (cells and platelets) suspended in an aqueous solution (plasma). This suspension behaves as a non-Newtonian fluid, meaning that its viscosity decreases with increasing shear stress. The RBCs, which are the main cellular component, behave as viscoelastic bodies since they readily deform and reform and also aggregate. Furthermore, the flow is affected by the size of the circulation vessel, ranging from >10 mm for larger veins and arteries down to as small as $\sim 5 \mu m$ in capillaries. Whole blood viscosity is also strongly influenced by the volume fraction of RBCs (the hematocrit), body temperature, and the plasma protein composition.^{51,52} Human blood outside the vascular system (*ex-vivo*) clots within 2–6 min after an injury, resulting from a complicated process called the coagulation cascade that takes place in the plasma. The process is highly regulated by coagulation factors such as fibrinogen and critically depends on free Ca^{2+} ions.^{53,54} During the coagulation process as a blood clot is formed, blood changes its properties from a viscoelastic fluid to a viscoelastic solid. The transition point between the two states is known as the gel point (GP). The time to arrive at the gel point (TGP) is a function of the shear stress, increasing with decreasing shear stress. Extrapolating from published values⁵⁵ for TGP vs. shear stress for the flow rate

conditions under capillary flow in nrLFA gives TGP values of 6 min or more. By comparison, the longest measurement time associated with the experiments presented here are 4–5 min, ensuring that no premature clot formation occurs.

This article focuses on the calibration and reproducibility of the flow of blood and other bodily fluids in nitrocellulose membranes that are the key component used in nrLFA, as well as a promising application of a simple POC blood coagulation self-monitoring device for patients with cardiovascular diseases who are undergoing anti-coagulation therapy. In addition to full blood testing at a doctor's office, clinic, or lab every few weeks, frequent self-testing for these patients is very important because it can significantly reduce the risk of stroke (by ~55%), major hemorrhage (~35%), and even death (~39%).⁵⁶

II. MATERIALS AND METHODS

A. Materials and chemicals

Membranes of several types of materials known to have well-behaved capillary properties were investigated (as shown in Table I): nitrocellulose (NC), nylon, cellulose acetate (CA), polyethersulfone (PES), and polyvinylidene difluoride (PVDF). NC membranes are widely utilized in commercial LFA applications. Although hydrophobic by nature, NC membranes are converted to exhibit hydrophilic surface properties using a surfactant, which allows the flow of aqueous sample solutions. NC membranes have a sufficiently high protein binding capability enabling effective immobilization of adequate amounts of primary and secondary antibodies in order to form test and control lines. However, balanced binding properties allow conjugated antibodies and antigens to pass through the membrane matrix after blocking⁷ and be captured by those lines. NC is directly cast on polyester backing, which significantly improves the handling properties of the NC membrane without interfering with its function.⁶ These features make NC membranes the most commonly utilized material for LFA. Nylon, CA, and PES membranes are widely utilized in micro- or nano-filtration and have various distinctive properties.⁵⁷ Nylon membranes are hydrophilic, highly solvent-resistant, and super-strong materials due to their regular and symmetrical molecular structure. They also have the highest protein binding capability among all four membrane materials. CA membranes are hydrophilic, low in

TABLE I. Materials used in the nrLFA and commercial sources. NC—nitrocellulose, CA—cellulose acetate, PES—polyethersulfone, and PVDF—polyvinylidene difluoride.

Purpose	Manufacturer	Model No.	Material	Comments
Analytical/filtration membrane	MilliporeSigma	HF075	NC	Fastest NC on market; ideal for whole blood LFA tests
	MilliporeSigma	HF135	NC	NC with moderate capillary flow rate; widely used in LFA tests
	MilliporeSigma	HF180	NC	Slowest NC on market; ideal for high sensitivity LFA tests
	Sartorius	CN95	NC	NC with moderate capillary flow rate; widely used in LFA tests
	Sartorius	CN140	NC	NC with moderate capillary flow rate; widely used in LFA tests
	Sterlitech	Nylon	Nylon	Hydrophilic, high protein binding, robust; microfiltration
	Sterlitech	CA	CA	Hydrophilic, low protein binding, high thermal stability; microfiltration
	Sterlitech	PES	PES	Hydrophilic, no surfactants, low protein binding; microfiltration
Sample Pad	MilliporeSigma	Durapore	PVDF	Hydrophilic, low protein binding; moderate capillary flow rate; microfiltration
	Ahlstrom	8950	Fiberglass	Low fluid retention; fast sample release; high tensile strength
Wicking Pad	Whatman	470	Cellulose	High absorbency; bio-degradable; low-cost

surface charge, and inexpensive to produce and have low protein binding capability but high thermal stability. PES membranes are hydrophilic, acid- and base-resistant, and have low protein binding capability and high capillary flow rate. PVDF membranes can be manufactured to be hydrophilic or hydrophobic depending on the chemical additives and manufacturing procedures that can alter physicochemical and microstructural features of the material.⁵⁸ Hydrophilic PVDF is chemical- and temperature-resistant and has low protein binding capability and moderate capillary flow rate, while hydrophobic PVDF has high protein binding capability and minimal capillary flow.⁵⁷ In general, filtration membranes have smaller pore sizes ($\sim 0.1\text{--}5\ \mu\text{m}$) than lateral flow membranes ($\sim 7\text{--}15\ \mu\text{m}$) due to their intended applications. The smaller pore size is suitable for protein transport but limits the transport of RBCs ($6\text{--}8\ \mu\text{m}$ in diameter, but pliable). CA, PES, and PVDF membranes of $5\ \mu\text{m}$ pore size and nylon membranes of $5\ \mu\text{m}$ and $10\ \mu\text{m}$ pore sizes were selected for property characterization to determine their potential use in whole blood assays. All selected membranes were hydrophilic.

Citrated rabbit whole blood was purchased from HemoStat Laboratories (Dixon, CA). According to the supplier, the volume ratio of rabbit whole blood to citrate solution [4% w/v trisodium citrate (MilliporeSigma) in water] is 4 to 1. This corresponds to a significant amount of sodium citrate beyond what is needed for Ca^{2+} ion immobilization.⁵³ Chemicals such as calcium chloride (CaCl_2), sodium chloride (NaCl), ammonium hydroxide (NH_4OH), glycerin, acetic acid, and lactic acid were purchased from Fisher Scientific (Pittsburgh, PA). Artificial sweat was prepared according to the standard ISO 3160-2,⁵⁹ which consists of 20 g/l NaCl , 17.5 g/l NH_4OH , 5 g/l acetic acid, and 15 g/l lactic acid in deionized (DI) water.

B. Fabrication of nrLFA device

Fig. 2(a) shows the configuration of the nrLFA device utilized for all the studies reported in this article. The device is based on a conventional LFA test strip and uses a plastic cassette

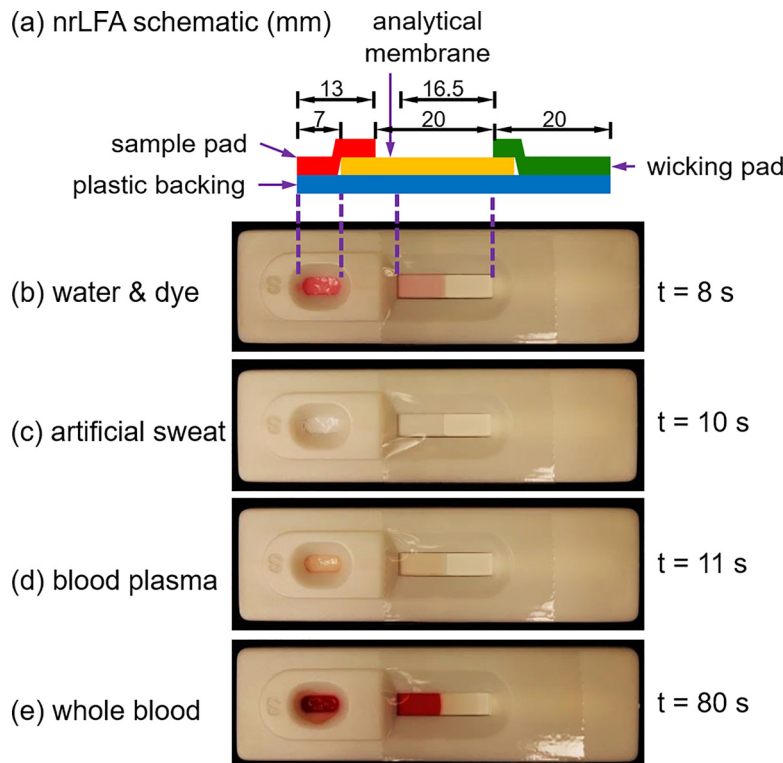


FIG. 2. nrLFA schematic (a) and photos of nrLFA devices with $30\ \mu\text{l}$ various fluid samples on HF075; (b) water and dye; (c) artificial sweat; (d) centrifuged blood plasma; and (e) whole blood. The time required to reach the same distance in each case is shown at right.

holder with a cut-out window that allows monitoring of flow within the strip. The nrLFA test strip includes a fiber glass sample pad (Ahlstrom, Helsinki, Finland), a NC lateral flow membrane (MilliporeSigma, Billerica, MA), a cellulose wicking pad (Whatman, Little Chalfont, United Kingdom), and a plastic backing card (Diagnostic Consulting Network, Carlsbad, CA). Unlike LFA, no conjugate pad is used for nrLFA. The overall strip dimension is 4 mm × 53 mm, and the lengths of the components are 13 mm for the sample pad, 30 mm for the analytical membrane, and 20 mm for the wicking pad. The overlaps of the analytical membrane with the sample pad and with the wicking pad are 6 and 4 mm, respectively. Long sheets of the three components are stacked and assembled on the plastic backing card and then cut into strips of 4 mm width using a CM4000 guillotine cutter (BioDot, Irvine, CA). The completed nrLFA strip is then placed inside a plastic cassette (Diagnostic Consulting Network, Carlsbad, CA), which consists of two plastic pieces that snap together. The cassette has a sample dispense opening and an observation window, with a length of 16.5 mm. The observation window was sealed using transparent tape to prevent the evaporation of sample fluid during testing. No reagent printing or membrane drying process is involved during the fabrication process.

During nrLFA tests, a camera and a timer were utilized to visually document the fluid travel distance with the fixed time interval (2 s). The starting point (distance $D=0$) was selected when the fluid just appeared in the observation window and the ending point ($D=16$ mm) was selected when the fluid front (furthest point of the rounded fluid front) reached 16 mm from the starting point. During the tests, after the sample fluid was dispensed on the nrLFA device, either the time needed to travel a certain distance or the distance traveled after a certain period of time was measured. Multiple tests were performed ($n=10$) to evaluate the reproducibility of nrLFA. The number of pixels associated with each fluid travel distance was obtained and then converted into the actual distance using Image J.⁶⁰ The mean and standard deviation of the travel distance were calculated using Excel. This method applies to all the tests mentioned in Sections III B–III E below.

Figs. 2(c)–2(e) show photos of nrLFA devices utilized for the evaluation of various bodily fluid samples. In all cases, fluid fronts are easily observable with the naked eye. For the solution-based samples—dye solution, artificial sweat, and centrifuged plasma (Figs. 2(b)–2(d))—the travel distance was roughly the same, indicating that the fluid flow is determined by the capillary property of water in the membrane. For the whole blood (“suspension”) case, Fig. 2(e) clearly shows the separation between the RBC front (red front) and the plasma front (light beige front), due to the filtration property of the nitrocellulose membrane. The plasma front traveled approximately twice the distance of the RBC front at $t=80$ s. The flow rate of the plasma component in whole blood is, however, much slower than that of the centrifuged plasma (discussed in Session III C).

C. Preparation of adjusted blood samples

Citrated whole blood (rabbit) with hematocrit (Hct) values of 25%, 30%, 35%, and 40% were obtained by extracting freshly separated plasma from low Hct blood (19%–25% for various batches from the supplier) after light centrifugation (Thermo Fisher Scientific accuSpin Micro 17, Osterode am Harz, Germany) at $400 \times g$ for 6 min, and then re-suspended by gentle agitation. Centrifuged plasma samples were obtained by centrifugation of citrated whole blood at $600 \times g$ for 10 min.

In nrLFA experiments with induced coagulation, samples comprised of 160 μ l of citrated rabbit blood, 5 μ l of 0.9% NaCl, and 15 μ l of 300 mM CaCl₂. For a control sample, the CaCl₂ solution was substituted with 15 μ l of 0.9% NaCl to maintain a consistent Hct in all samples. All solutions were maintained at 39 °C. After combining all components, the experimental mixture was pre-incubated for 2 min at 39 °C to allow initiation of the blood coagulation process before dispensing a volume of 30 μ l into the nrLFA inlet port.

D. Viscosity measurement

Viscosity of each sample was measured ($n=3$) using a falling-ball viscometer (Gilmont Instruments Viscometer 08701-00, Barrington, IL) at room temperature (19–20 °C). The average value was calculated and utilized in Section III C.

III. RESULTS AND DISCUSSION

A. Membrane characterization

Table II shows basic properties of the various membranes that were investigated. The membrane thickness and basis weight are measured and calculated without including polyester backing material. The membrane porosity expressed as % of empty space in the overall membrane matrix was measured using the water-saturation method: porosity = [(weight of saturated sample) – (weight of dry sample)]/(density of water)/(volume of sample matrix) × 100%. The values included in Table II reflect the ratio of the absorbed water volume (absorbed water mass/water density) to the membrane matrix volume (membrane area × membrane thickness). The capillary rise time (mean ± standard deviation) of each membrane was measured for a distance of 4 cm using a standard capillary flow test stand⁶¹ (more information can be found in Fig. S1 in the [supplementary material](#)). The capillary flow rate was calculated from the mean capillary rise time values. All measurements were performed in triplicate ($n=3$).

As shown in Table II, MilliporeSigma (Billerica, MA) High-FlowTM Plus membranes (HF075, HF135, and HF180) have similar materials properties such as thickness, basis weight, and porosity. The difference in capillary rise time and equivalent flow rate is due to the differences in pore size (with larger but fewer pores for faster membranes vs. slower membranes with smaller but more pores), which are achieved mainly by changing fabrication conditions⁶¹ (e.g., selection of solvents and non-solvents or precipitation rate of nitrocellulose lacquer) (more information can be found in Fig. S2 in the [supplementary material](#)). HF075 has the fastest capillary rise time and highest capillary flow rate, followed by HF135 with moderate capillary rise time and capillary flow rate, and HF180 which has the longest capillary rise time and lowest capillary flow rate. Sartorius (Göttingen, Germany) membranes CN95 and CN140 have slightly different membrane thicknesses and basis weights (less than 20% difference) and significantly different capillary rise times and capillary flow rates (more than 50% difference).

Despite reported concerns of inconsistency in flow characteristics,⁷ the NC membranes tested in this study from two different manufacturers all exhibited narrow capillary rise time

TABLE II. Measured properties of various membranes.

Membrane Type	Membrane thickness (μm)	Basis weight (mg/cm^2)	Density (g/cm^3)	Porosity (%)	Pore size (μm)	Capillary rise time ^a (s/4 cm)	Capillary flow rate ^b (mm/s)
HF075 ^c	147	3.40	0.231	82.4	14.5 ^d	77 ± 2	0.52
HF135 ^c	145	3.50	0.241	82.8	11.6 ^d	146 ± 3	0.27
HF180 ^c	143	3.59	0.251	78.9	8.6 ^d	154 ± 4	0.26
CN95 ^c	155	4.41	0.285	82.0	15 ^e	87 ± 2	0.50
CN140 ^c	135	3.58	0.265	80.4	10 ^e	136 ± 2	0.29
Nylon	105	4.73	0.450	61.9	10 ^e	210 ± 14	0.19
Nylon	103	4.47	0.434	68.4	5 ^e	334 ± 26	0.12
CA	89	3.93	0.442	40.3	5 ^e	457 ± 32	0.09
PES	135	3.57	0.264	75.9	5 ^e	49 ± 1	0.82
Durapore	134	7.90	0.590	49.4	5 ^e	149 ± 5	0.27

^aMean ± SD for $n=3$.

^bEffective flow rate for travel of 4 cm.

^cMembranes with polyester backing.

^dMean for $n=20$.

^eLiterature values.

distribution. However, occasionally an offset in capillary rise time was observed among some NC membranes compared to manufacturers' specification. For example, for HF180 the capillary rise time is specified as 180 ± 45 s/4 cm, in other words ranging from 135 to 225 s. Interestingly, our corresponding measurements ranged from 150 to 158 s or 154 ± 4 s/4 cm, which is within the overall specification but with a much tighter distribution. Nylon, CA, PES, and PVDF membranes from Sterlitech (Kent, WA) are non-backed membranes intended for smaller molecule assays, filtration, and purification purposes. Nylon and CA have a much wider range of capillary rise time and much slower capillary flow rate than NC membranes that are intended for lateral flow tests. Interestingly, PES exhibits one of the tightest ranges of capillary rise time and fastest capillary flow rate with an aqueous sample solution among all the membranes listed in Table II.

Several types of membranes were evaluated using whole blood: NC, nylon, CA, PES, and PVDF. As shown in Fig. S3 in the [supplementary material](#), the NC membranes provide optimum performance: uniform flow, wide range of flow rates based on different pore sizes, and clear separation of RBCs and plasma. The flow of whole blood in several membranes (nylon, CA, PES, and PVDF) has been found to be unsatisfactory for our application (also shown in Fig. S3, [supplementary material](#)), and therefore it is not investigated further.

B. Flow comparison of various membranes

Flow properties of widely used analytical membranes were tested on the nrLFA device. MilliporeSigma nitrocellulose membranes were tested using $30 \mu\text{L}$ DI water or centrifuged plasma ($n = 10$). The membranes produced the following capillary rise times for a 4 cm travel: HF075 – 77 ± 2 s, HF135 – 146 ± 3 s, and HF180 – 154 ± 4 s (Table II).

Fig. 3 shows the flow properties of MilliporeSigma HF075, HF135, and HF180 membranes in nrLFA devices. As expected, the flow rates of DI water and centrifuged plasma (abbreviated as W and P in Fig. 3) are slowest on HF180, moderate on HF135, and fastest on HF075. The difference between DI water and plasma travel distance becomes larger when the membrane has a slower flow rate, and vice versa. For travel of 12 mm on the nrLFA device, the time difference between plasma and DI water is ~ 5 s on HF075 and ~ 13 s on HF135 and HF180. The results demonstrate that membranes with a slower flow rate can distinguish the difference in fluid viscosity more effectively than membranes with a faster flow rate. However, in ultimate use as a blood coagulation monitoring device, the shorter test time enabled by the faster flow rate of HF075 is probably a deciding consideration.

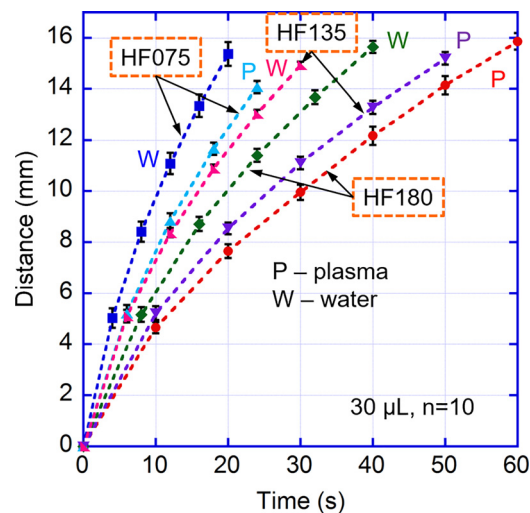


FIG. 3. Flow property comparison of various membranes using DI water and centrifuged plasma.

C. nrLFA reproducibility tests

Experiments were conducted to test the reproducibility of the nrLFA device using several bodily fluids: citrated whole blood (WB), centrifuged plasma, and artificial sweat. In addition, two fluids were used for calibration and comparison: DI water and 50% v/v glycerin in water solution (GW50), which has a viscosity (~ 7.6 cP) similar to that of whole blood measured^{51,62} at low shear rate *ex-vivo* (~ 23 °C). Standard sample volumes of 30 μl and 100 μl were selected, which are consistent with volume limits of commercial capillary blood collection tubes. Reproducibility tests with each sample fluid were performed ($n = 10$) to evaluate device reproducibility. For citrated whole blood samples, the Hct was measured to be 25%.

Table III shows the time (mean \pm standard deviation) for various fluid fronts to travel 16 mm on the nrLFA device and the coefficient of variation (CV – standard deviation divided by mean $\times 100\%$). Washburn's equation⁶³ describing capillary rise of a liquid in a tube indicates the well-known square law relationship between travel distance (L) and flow time (t)

$$L^2 = \frac{(\gamma D_t t) \cos \theta}{4\mu},$$

where D_t is the tube diameter, θ is the contact angle between the fluid and the membrane, and γ and μ are the fluid surface tension and viscosity. Capillary flow in a dry porous medium (so-called *wet-out* flow), such as the NC membrane in nrLFA, can be modeled by the equivalent Darcy's law⁶⁴ using an average pore diameter D_p combined with the tortuosity c of the medium

$$L^2 = \frac{(\gamma c D_p t) \cos \theta}{4\mu}.$$

As expected, the dynamic fluid flow rate (dL/dt) is proportional to the pore diameter. The flow rate is also inversely proportional to its viscosity – fluid with higher viscosity travels slower, and vice versa. The water contact angle (WCA) on the various membranes was investigated. The WCA was found to be difficult to measure accurately because of the rapid spread of the fluid on the membrane surface. The WCA immediately after droplet dispense is shown in the [supplementary material](#) (Fig. S4). Interestingly, the contact angles showed a bell-shaped distribution versus the capillary rise time. In most cases, the same membrane material (e.g., nylon and NC) but with different rise times showed similar contact angle values. This is probably because membranes made from the same material have both the same intrinsic surface properties and a similar microscopic structure. Although the nitrocellulose polymer itself is hydrophobic, NC membranes (HF and CN series) show low contact angle and short capillary rise time due to the addition of surfactants. As shown in Table III, for samples of both 30 μl and 100 μl of water, artificial sweat, centrifuged plasma, and GW50 solution, fluids with higher viscosity exhibited increasingly longer travel time, consistent with Washburn's equation. The plasma

TABLE III. Time to travel 16 mm on nrLFA device (HF075) using 30 and 100 μl sample volumes ($n = 10$).

Sample fluids	30 μl		100 μl	
	Time to travel 16 mm (s) (Mean \pm SD)	Variation (CV ^a) (%)	Time to travel 16 mm (s) (Mean \pm SD)	Variation (CV ^a) (%)
Water (1.16 cP)	21 \pm 1	5	20 \pm 1	5
GW 50% (7.59 cP)	120 \pm 8	5	120 \pm 5	4
WB (RBC front)	235 \pm 6	3	225 \pm 7	3
WB (plasma front)	98 \pm 3	3	93 \pm 4	4
Plasma Only (1.93 cP)	29 \pm 1	3	29 \pm 1	3
Artif. Sweat (1.30 cP)	27 \pm 1	4	26 \pm 1	4

^aCV = SD/Mean $\times 100\%$.

exhibited different effective viscosities when it was traveling as a component in whole blood, and by itself as (centrifuged) plasma. Not unexpectedly, the flow rate of plasma as a component in whole blood is much slower than that of plasma-only because highly packed cellular components (such as RBCs and WBCs) on the nrLFA strip increase the flow resistance of plasma through the strip. The same situation is likely to occur during the flow of other complex biological fluids where the flow rate of the aqueous component will be reduced by the flow resistance from slower moving cellular components. Consistent with this hypothesis, the RBC front had the longest travel time due to the high effective viscosity of packed RBCs.

The coefficient of variation (CV) is a standardized measure of dispersion of a probability distribution and is widely utilized for quality control purpose to determine the precision of *in vitro* diagnostic devices (IVDs), indicating the agreement between independent diagnostic test results obtained under stipulated conditions. For example, the FDA has used a precision criterion of $CV < 10\%$ for an IVD used in the measurement of C-reactive protein assay.⁶⁵ It is instructive to compare the reproducibility of the results with the nrLFA device when using various bodily fluids to the specifications given by the membrane manufacturers, which is typically a variation in capillary rise time of the order of $\pm 25\%$. As shown in Table III, all fluid flows exhibit small CVs ranging from 3% to 5%, with little influence of using $30\ \mu\text{L}$ and $100\ \mu\text{L}$ sample volumes. Since the images of fluid flow were captured once every 2 s (30 frames per minute) by the camera and the time to travel 16 mm was manually calculated using two adjacent data points, travel time variations of fluids with low viscosity are very close to the detection limit. The variation values can be further reduced if a detection method with higher time resolution is utilized, such as video recording. The results demonstrate that with all nrLFA strip components attached and the strip assembled into the cassette, the overall nrLFA device exhibits excellent reproducibility of fluid flow, exceeding membrane manufacturers' specification. Since we have shown that there is good correlation between accuracy of water flow time and RBC front flow time, the proper performance of the nrLFA device can be easily tested using water as the sample, confirming the capillary flow time. Given the high level of reproducibility of membrane properties, a single calibration per batch of strips is likely to be sufficient to validate the test results.

Fig. 4 shows the travel distance over time for $30\ \mu\text{L}$ and $100\ \mu\text{L}$ sample volumes. As can be seen, both sample volumes exhibit very similar standard deviations for water, centrifuged plasma, and plasma in whole blood. Artificial sweat exhibits a slightly smaller standard deviation for the $30\ \mu\text{L}$ case, while GW50 solution exhibits a slightly smaller standard deviation for the $100\ \mu\text{L}$ case. Interestingly, the travel of RBCs in whole blood exhibits the smallest standard deviation for both volumes. Overall, both $30\ \mu\text{L}$ and $100\ \mu\text{L}$ sample volumes give comparable standard deviations when using various fluids, and both volumes are appropriate to be used on the nrLFA device.

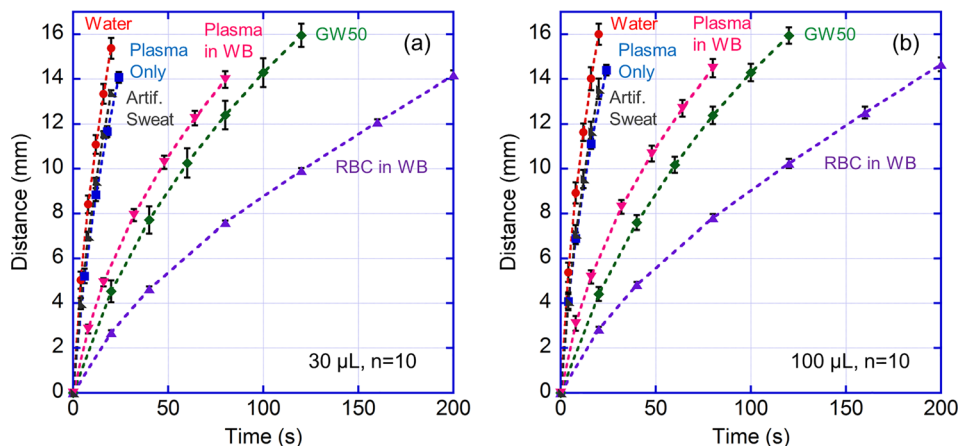


FIG. 4. Average distance (and standard deviation) vs. time for various fluids with sample volume of: (a) $30\ \mu\text{L}$ and (b) $100\ \mu\text{L}$ on the nrLFA device (HF075).

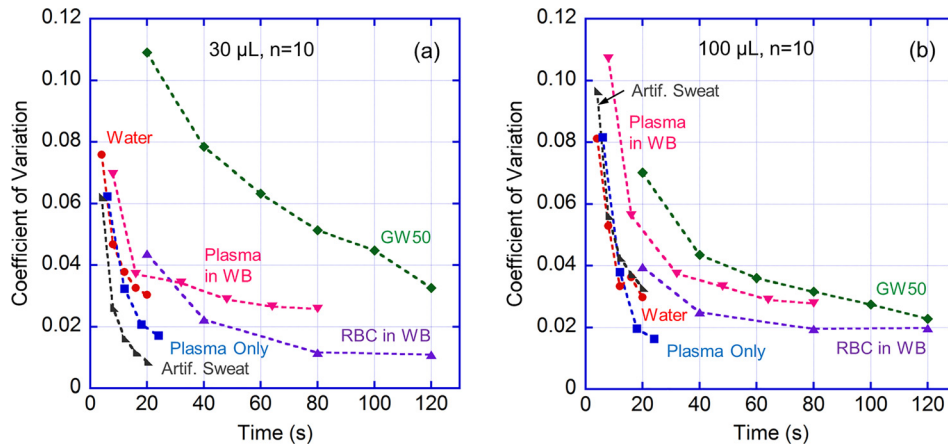


FIG. 5. Coefficient variation vs. time for various fluids with sample volume of: (a) 30 μL ; and (b) 100 μL on the nrLFA device (HF075).

Fig. 5 shows the change in CV as a function of flow time for various fluids. When using 30 μL sample only GW50 solution had a CV exceeding 10%, and in the case of 100 μL samples only plasma in whole blood had a CV > 10%, both at the beginning of the test ($t < 30\text{ s}$). At $t \geq 60\text{ s}$, CV < 7% with 30 μL sample and < 4% with 100 μL sample were achieved. Most importantly, at $t = 80\text{ s}$, RBC flow in whole blood had a CV of 1% for the 30 μL sample and 2% for the 100 μL sample. For comparison, the commercial blood coagulation analyzer CoaguCheck XS from Roche Diagnostics is reported to have CV of 2% when using venous blood and 3.4% when using capillary blood,⁶⁶ which is slightly higher than the 1.0%–2.0% CV obtained for RBC flow on the nrLFA. This result demonstrates that the nrLFA device exhibits excellent reproducibility and thus has solid promise for future commercialization.

D. Study of hematocrit and volume effect

The effects of hematocrit and sample volume on fluid travel distance on the nrLFA device were also investigated. In the hematocrit study, citrated whole blood samples adjusted to three different Hct values were utilized. During the tests, 30 μL blood samples were dispensed on the nrLFA devices and the travel distances of both RBC and plasma fronts were measured. To study the effect of the sample volume on the travel distance, DI water samples ranging from 10 to 100 μL were examined ($n = 10$) on the nrLFA device using HF075.

Fig. 6(a) shows fluid travel distance vs. time for Hct values of 25%, 30%, 35%, and 40%. As can be seen, for both RBC and plasma fronts the travel distance decreases monotonically with increasing Hct, indicating a reduction in flow rate. Fig. 6(b) shows fluid travel distance vs. Hct values for travel times of 80 s and 160 s. At $t = 80\text{ s}$, plasma in citrated whole blood traveled $\sim 14\text{ mm}$ for 25% Hct, $\sim 13\text{ mm}$ for 30% Hct, $\sim 11\text{ mm}$ for 35% Hct, and $\sim 8.5\text{ mm}$ for 40% Hct, which was approximately twice the distance that RBCs traveled at that moment. At $t = 160\text{ s}$, RBCs in citrated whole blood traveled $\sim 12\text{ mm}$ for 25% Hct, $\sim 11\text{ mm}$ for 30% Hct, $\sim 9.5\text{ mm}$ for 35% Hct, and $\sim 8\text{ mm}$ for 40% Hct. Standard deviations of all eight fronts are quite consistent compared to Fig. 4. The result demonstrates that increasing hematocrit elevates the effective viscosity of both plasma and cellular components in citrated whole blood, and thus both components travel a shorter distance for a given time on the nrLFA device.

Fig. 7 shows the fluid travel distance over time using several volumes of DI water: 10, 15, 20, 30, and 100 μL . As shown in Fig. 7(a), all volumes of DI water reach the end of observation window ($D = 16.5\text{ mm}$) except the 10 μL case. Comparing at a fixed time of $t = 16\text{ s}$, the fluid travel distance increases significantly as the sample volume increases from 10 μL to 20 μL , moderately from 20 μL to 30 μL , and only slightly from 30 μL to 100 μL , as can be seen in Fig. 7(b). This effect is probably due to the increasing sample volume fully saturating sample pad that results in efficient fluid transfer to the analytical membrane. Another possible factor could be

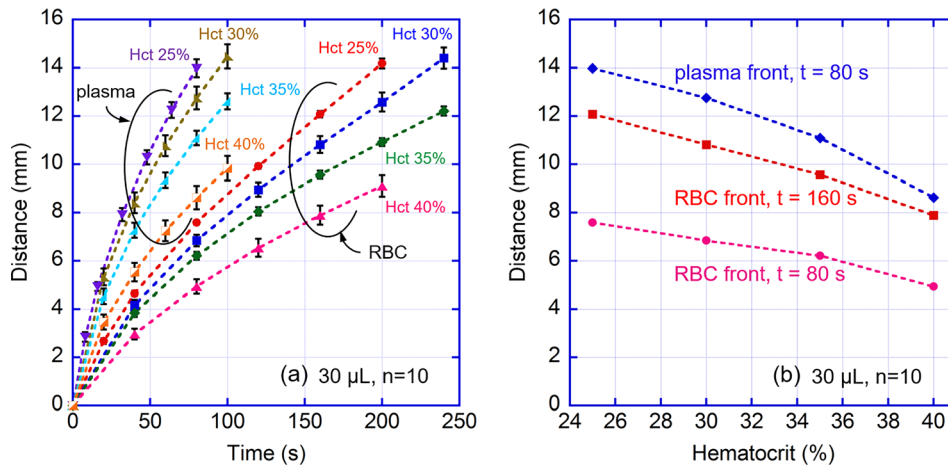


FIG. 6. Relationship between travel distance and hematocrit when using citrated whole blood adjusted to different Hct values: (a) travel distance vs. time for both RBC and plasma fronts and (b) travel distance vs. Hct for RBC front at $t = 80$ s and $t = 160$ s and plasma front at $t = 80$ s on nrLFA device (HF075).

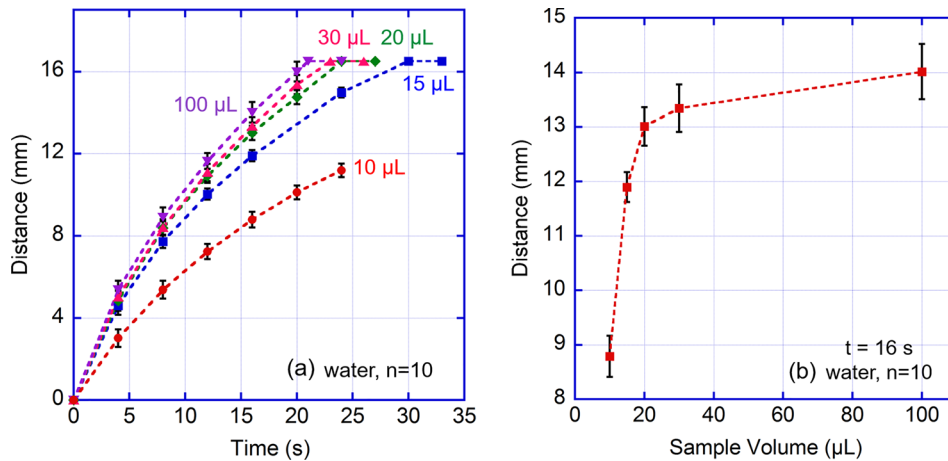


FIG. 7. Relationship between the travel distance and sample volume when using various volumes of DI water: (a) travel distance vs. time and (b) travel distance vs. sample volume for the fixed time of 16 s on the nrLFA device (HF075).

the larger input pressure on the sample pad due to gravity thus increasing the pressure gradient between inlet and outlet and leading to faster fluid flow on the analytical membrane. However, as the sample volume increases beyond $\sim 30 \mu\text{L}$, the ability of the membrane to transport the fluid becomes the limiting factor. Since the increase in sample volume in the 10 to $20 \mu\text{L}$ range has a significant effect on travel distance, the minimum sample volume for reproducible results with the current nrLFA device is $\sim 20 \mu\text{L}$ to ensure that slight variation in sample volume during clinical applications does not result in significant differences in tests results.

E. Reproducibility of coagulation tests

Since one of the potential clinical applications of the nrLFA device is blood coagulation monitoring for patients on anti-coagulation therapy, it is critical to evaluate device reproducibility when the coagulation process is introduced on the device. During this aspect of the study, HF075 was utilized as the analytical membrane, and coagulation-activated citrated blood was utilized to mimic real blood sample from patients ($n = 10$). Citrated blood does not coagulate because of the absence of free Ca^{2+} ions. By adding CaCl_2 solution into citrated blood, the resulting free Ca^{2+} ions reactivate the coagulation process. An anti-coagulated control test was

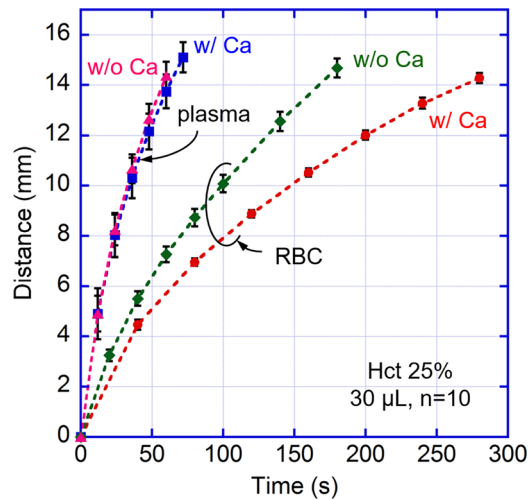


FIG. 8. Travel distance of plasma and RBC fronts in citrated whole blood vs. time with and without 300 mM CaCl_2 on the nrLFA device (HF075).

also conducted ($n = 10$) in which the same volume of 0.9% NaCl solution was added to citrated blood replacing the CaCl_2 solution. The Hct of citrated whole blood was measured to be 25% in both tests.

Fig. 8 shows RBC and plasma travel distance over time with and without addition of 300 mM CaCl_2 . The presence of Ca^{2+} ions in the blood sample, which leads to the activation of blood coagulation, caused only a slight decrease in the plasma travel distance. In contrast, a significant decrease in RBC travel distance was observed when the coagulation process was activated. The probable reason is that the plasma front travels fast enough compared to the rate of coagulation such that it reaches the end of observation window before enough fibrin clots can be formed to slow down its flow rate. Since the RBCs travel much slower, the gradual formation of fibrin clots can reduce their flow rate significantly. At $t = 180$ s, RBCs travel ~ 11 mm with CaCl_2 solution compared to ~ 15 mm without CaCl_2 solution.

It is interesting to compare the effect of CaCl_2 addition on blood flow (Fig. 8) with the effect of Hct (Fig. 6), since in practice it is important to be able to distinguish between these two effects in order to properly interpret the test results. Since the effect of Ca^{2+} ions on plasma flow is very minor (under the specific geometry of the current test strip and cassette), changes observed in plasma flow can be attributed to variations in Hct. This information can then be used to calibrate changes observed in RBC flow conditions (which are sensitive to both effects) in order to extract the coagulation conditions.

Finally, regarding flow reproducibility with the addition of 300 mM CaCl_2 , the CV of the plasma front at $t = 60$ s is 5% and the CV of the RBC front at $t = 240$ s is 2%. Clearly, the nrLFA device exhibits excellent reproducibility when the coagulation process is activated on the test strip.

IV. SUMMARY AND CONCLUSIONS

In summary, reproducibility of nrLFA devices and their potential application in a whole blood assay have been reported. nrLFA devices exhibit good reproducibility in fluid flow using both 30 μl and 100 μl sample volumes ($t = 60$ s, $\text{CV} < 7\%$ for 30 μl and $\text{CV} < 4\%$ for 100 μl) probably due to the absence of additional chemicals used during the fabrication process of conventional LFA devices (e.g., immobilization of immune-reactive reagents, blocking of undesired binding sites on membrane, and surface treatment with surfactants). Multiple membrane types of different materials and with various properties were characterized. MilliporeSigma HF075, HF135, and HF180 membranes demonstrated properties with high suitability for nrLFA devices and exhibited good reproducibility. The effects of different hematocrit values (25%–40%) in

whole blood and sample volume (10–100 μl) were also investigated. Higher hematocrit values result in higher effective viscosity of both plasma and RBC components in whole blood on the nrLFA device, due to the effect of highly concentrated RBCs within the membrane. The minimum sample volume of the device to ensure test accuracy is $\sim 20 \mu\text{l}$ for the current assay design. Most importantly, blood coagulation tests performed on the nrLFA device demonstrated excellent reproducibility, with 5% CV for the plasma front at $t = 60 \text{ s}$ and 2% CV for RBC front at $t = 240 \text{ s}$.

Future nrLFA improvements include reducing the blood sample volume to be in the range of fluid available from a conventional finger prick (10–20 μl), optimizing the design of the cassette, and conducting healthy volunteer tests and clinical trials that would validate the results for human subjects.

The nrLFA device displays strong potential for commercialization as a point-of-care monitoring of blood coagulation conditions by being easy to fabricate, simple to operate, cheap to use, and high in reproducibility. Other potential applications include the analysis of blood hematocrit and hemoglobin and the effect of biomarkers on transport of plasma, sweat, and other bodily fluids. Finally, the flow characterization of bodily fluids in various membranes provided by this study can be of use for the future development of wearable sensors for a variety of recreational, industrial, and military applications.

SUPPLEMENTARY MATERIAL

See [supplementary material](#) for a summary of commercial POC blood analyzers, capillary rise time measurement, pore size information of MilliporeSigma NC membranes, and flow of whole blood and WCA measurement on various filtration membranes.

ACKNOWLEDGMENTS

This research was supported by the National Science Foundation (PFI:AIR Award No. #1500236) and the University Research Council Interdisciplinary Program from the University of Cincinnati. We thank M. A. Mansfield from MilliporeSigma for many useful discussions regarding nitrocellulose membranes, Roy Chung from Diagnostics Consulting Network for providing insight on membrane selection and LFA operation, and Prajokta Ray of the UC NanoLab for providing artificial sweat.

- ¹Z. Li, Y. Wang, J. Wang, Z. Tang, J. G. Pounds, and Y. Lin, *Anal. Chem.* **82**(16), 7008–7014 (2010).
- ²Z. Yan, L. Zhou, Y. Zhao, J. Wang, L. Huang, K. Hu, H. Liu, H. Wang, Z. Guo, Y. Song, H. Huang, and R. Yang, *Sens. Actuators, B* **119**(2), 656–663 (2006).
- ³K. Ching, X. He, L. Stanker, A. Lin, J. McGarvey, and R. Hnasko, *Toxins* **7**(4), 1163 (2015).
- ⁴H. Kuang, C. Xing, C. Hao, L. Liu, L. Wang, and C. Xu, *Sensors* **13**(4), 4214 (2013).
- ⁵C. Liu, Q. Jia, C. Yang, R. Qiao, L. Jing, L. Wang, C. Xu, and M. Gao, *Anal. Chem.* **83**(17), 6778–6784 (2011).
- ⁶M. A. Mansfield, in *Drugs of Abuse: Body Fluid Testing*, edited by R. C. Wong and H. Y. Tse (Humana Press, Totowa, NJ, 2005), pp. 71–85.
- ⁷M. A. Mansfield, in *Lateral Flow Immunoassay*, edited by R. Wong and H. Tse (Humana Press, Totowa, NJ, 2009), pp. 1–19.
- ⁸G. E. Fridley, C. A. Holstein, S. B. Oza, and P. Yager, *MRS Bull.* **38**(4), 326–330 (2013).
- ⁹A. W. Martinez, S. T. Phillips, M. J. Butte, and G. M. Whitesides, *Angew. Chem., Int. Ed.* **46**(8), 1318–1320 (2007).
- ¹⁰E. Carrilho, A. W. Martinez, and G. M. Whitesides, *Anal. Chem.* **81**(16), 7091–7095 (2009).
- ¹¹D. M. Cate, J. A. Adkins, J. Mettakoonpitak, and C. S. Henry, *Anal. Chem.* **87**(1), 19–41 (2015).
- ¹²V. Leung, “Development of paper-based devices for diagnostics and biosensing,” Master’s thesis, McMaster University, 2011.
- ¹³X. Li, D. R. Ballerini, and W. Shen, *Biomicrofluidics* **6**(1), 011301 (2012).
- ¹⁴X. Li, J. Tian, and W. Shen, *Cellulose* **17**(3), 649–659 (2010).
- ¹⁵C. Parolo and A. Merkoci, *Chem. Soc. Rev.* **42**(2), 450–457 (2013).
- ¹⁶A. K. Yetisen, M. S. Akram, and C. R. Lowe, *Lab Chip* **13**(12), 2210–2251 (2013).
- ¹⁷A. W. Martinez, S. T. Phillips, G. M. Whitesides, and E. Carrilho, *Anal. Chem.* **82**(1), 3–10 (2010).
- ¹⁸N. A. Meredith, C. Quinn, D. M. Cate, T. H. Reilly, J. Volckens, and C. S. Henry, *Analyst* **141**(6), 1874–1887 (2016).
- ¹⁹M. Medina-Sánchez, M. Cadevall, J. Ros, and A. Merkoçi, *Anal. Bioanal. Chem.* **407**(28), 8445–8449 (2015).
- ²⁰E. J. Maxwell, A. D. Mazzeo, and G. M. Whitesides, *MRS Bull.* **38**(04), 309–314 (2013).
- ²¹D. Tobjörk and R. Österbacka, *Adv. Mater.* **23**(17), 1935–1961 (2011).
- ²²A. Steckl, in *IEEE Spectrum* (IEEE, 2013), pp. 48–61.
- ²³M. Irimia-Vladu, *Chem. Soc. Rev.* **43**(2), 588–610 (2014).

- ²⁴S. Ahmed, M.-P. N. Bui, and A. Abbas, *Biosens. Bioelectron.* **77**, 249–263 (2016).
- ²⁵C. Desmet, C. A. Marquette, L. J. Blum, and B. Doumèche, *Biosens. Bioelectron.* **76**, 145–163 (2016).
- ²⁶J. L. Delaney, C. F. Hogan, J. Tian, and W. Shen, *Anal. Chem.* **83**(4), 1300–1306 (2011).
- ²⁷A. K. Ellerbee, S. T. Phillips, A. C. Siegel, K. A. Mirica, A. W. Martinez, P. Striehl, N. Jain, M. Prentiss, and G. M. Whitesides, *Anal. Chem.* **81**(20), 8447–8452 (2009).
- ²⁸X. Liu, M. Mwangi, X. Li, M. O'Brien, and G. M. Whitesides, *Lab Chip* **11**(13), 2189–2196 (2011).
- ²⁹Z. Nie, C. A. Nijhuis, J. Gong, X. Chen, A. Kumachev, A. W. Martinez, M. Narovlyansky, and G. M. Whitesides, *Lab Chip* **10**(4), 477–483 (2010).
- ³⁰S. Lee, A. J. Aranyosi, M. D. Wong, J. H. Hong, J. Lowe, C. Chan, D. Garlock, S. Shaw, P. D. Beattie, Z. Kratochvil, N. Kubasti, K. Seagers, R. Ghaffari, and C. D. Swanson, *Biosens. Bioelectron.* **78**, 290–299 (2016).
- ³¹E. M. Fenton, M. R. Mascarenas, G. P. López, and S. S. Sibbett, *ACS Appl. Mater. Interfaces* **1**(1), 124–129 (2009).
- ³²E. W. Nery and L. T. Kubota, *Anal. Bioanal. Chem.* **405**(24), 7573–7595 (2013).
- ³³E. Fu, B. Lutz, P. Kauffman, and P. Yager, *Lab Chip* **10**(7), 918–920 (2010).
- ³⁴H. Liu and R. M. Crooks, *J. Am. Chem. Soc.* **133**(44), 17564–17566 (2011).
- ³⁵A. T. Jafry, H. Lim, S. I. Kang, J. W. Suk, and J. Lee, *Colloids Surf., A* **492**, 190–198 (2016).
- ³⁶E. Fu, T. Liang, J. Houghtaling, S. Ramachandran, S. A. Ramsey, B. Lutz, and P. Yager, *Anal. Chem.* **83**(20), 7941–7946 (2011).
- ³⁷A. W. Martinez, S. T. Phillips, and G. M. Whitesides, *Proc. Natl. Acad. Sci. U.S.A.* **105**(50), 19606–19611 (2008).
- ³⁸B. J. Toley, J. A. Wang, M. Gupta, J. R. Buser, L. K. Laffeur, B. R. Lutz, E. Fu, and P. Yager, *Lab Chip* **15**(6), 1432–1444 (2015).
- ³⁹H. Li, D. Han, G. M. Pualetti, and A. J. Steckl, *Lab Chip* **14**(20), 4035–4041 (2014).
- ⁴⁰L. J. Stoot, N. A. Cairns, F. Cull, J. J. Taylor, J. D. Jeffrey, F. Morin, J. W. Mandelman, T. D. Clark, and S. J. Cooke, *Conserv. Physiol.* **2**(1), cou11 (2014).
- ⁴¹A. St John and C. P. Price, *Clin. Biochem. Rev.* **35**(3), 155–167 (2014).
- ⁴²E. Elizalde, R. Urteaga, and C. L. A. Berli, *Microfluid. Nanofluid.* **20**(10), 135–143 (2016).
- ⁴³H. H. Billett, *Clinical Methods: The History, Physical, and Laboratory Examinations*, 3rd ed. (Butterworths, Boston, 1990).
- ⁴⁴D. U. Silverthorn and B. R. Johnson, *Human Physiology: An Integrated Approach* (Pearson/Benjamin Cummings, San Francisco, 2010), pp. 535–546.
- ⁴⁵G. Chen, L. Zhao, Y. Liu, F. Liao, D. Han, and H. Zhou, *Chin. Sci. Bull.* **57**(16), 1946–1952 (2012).
- ⁴⁶H. W. Hou, A. A. S. Bhagat, W. C. Lee, S. Huang, J. Han, and C. T. Lim, *Micromachines* **2**(3), 319–343 (2011).
- ⁴⁷J. Shim, A. Browne, and C. Ahn, *Biomed. Microdevices* **12**(5), 949–957 (2010).
- ⁴⁸X. Yang, O. Forouzan, T. P. Brown, and S. S. Shevkoplyas, *Lab Chip* **12**(2), 274–280 (2012).
- ⁴⁹M. Toner and D. Irimia, *Annu. Rev. Biomed. Eng.* **7**(1), 77–103 (2005).
- ⁵⁰O. K. Baskurt and H. J. Meiselman, *Semin. Thromb. Hemostasis* **29**(5), 435–450 (2003).
- ⁵¹D. M. Eckmann, S. Bowers, M. Stecker, and A. T. Cheung, *Anesth. Analg.* **91**(3), 539–545 (2000).
- ⁵²S. Chien, S. Usami, H. M. Taylor, J. L. Lundberg, and M. I. Gregersen, *J. Appl. Physiol.* **21**(1), 81–87 (1966).
- ⁵³D. G. Bjoraker and T. R. Ketcham, *Thromb. Res.* **24**(5–6), 505–508 (1981).
- ⁵⁴E. P. Brass, W. B. Forman, R. V. Edwards, and O. Lindan, *Blood* **52**(4), 654–658 (1978).
- ⁵⁵M. Ranucci, T. Laddomada, M. Ranucci, and E. Baryshnikova, *Physiol. Rep.* **2**(7), 1–7 (2014).
- ⁵⁶C. Heneghan, P. Alonso-Coello, J. M. Garcia-Alamino, R. Perera, E. Meats, and P. Glasziou, *Lancet* **367**(9508), 404–411 (2006).
- ⁵⁷T. D. Brock, *Membrane Filtration: A User's Guide and Reference Manual* (Science Tech, 1983).
- ⁵⁸E. Fontananova, M. A. Bahattab, S. A. Aljlil, M. Alowairdy, G. Rinaldi, D. Vuono, J. B. Nagy, E. Drioli, and G. Di Profio, *RSC Adv.* **5**(69), 56219–56231 (2015).
- ⁵⁹ISO 3160-2: Watch-Cases and Accessories—Gold Alloy Coverings—Part 2: Determination of fineness, Thickness, Corrosion Resistance and Adhesion, 2015.
- ⁶⁰See <https://imagej.nih.gov/ij/> for Image Processing and Analysis in Java.
- ⁶¹M. A. Mansfield, private communication (2016).
- ⁶²G. A. M. Pop, D. J. Duncker, M. Gardien, P. Vranckx, S. Versluis, D. Hasan, and C. J. Slager, *Netherlands Heart J.* **10**(12), 512–516 (2002).
- ⁶³E. W. Washburn, *Phys. Rev.* **17**(3), 273–283 (1921).
- ⁶⁴M. F. Pucci, P. J. Liotier, and S. Drapier, in 20th International Conference on Composite Materials, Copenhagen, July 2015.
- ⁶⁵See <http://www.fda.gov/MedicalDevices/ucm077167.htm> for Guidance for Industry - Review Criteria for Assessment of C Reactive Protein (CRP), High Sensitivity C-Reactive Protein (hsCRP) and Cardiac C-Reactive Protein (cCRP) Assays, FDA (2005).
- ⁶⁶CoaguChek[®] XS PT Test Package Insert.